Journal of BUON **9:** 451-464, 2004

ORIGINAL ARTICLE

A comparison of Monte Carlo simulation with experimental dosimetric techniques for a 6 MV stereotactic radiotherapy unit

I. Tsougos[1], K. Theodorou[1], M.A. Bazioglou[2], S. Stathakis[1], C. Kappas[1]

[1]Department of Medical Physics, Medical School, University of Thessaly, Larissa, Hellas; [2]Department of Medical Physics, Medical School, University of Ioannina, Ioannina, Hellas

Summary

Purpose: *To compare Monte Carlo simulation with conventional dosimetry techniques for stereotactic radiotherapy (SRT), since accurate dosimetry of narrow photon beams is very complicated and has often been questioned, mainly due to the lack of lateral electronic equilibrium and uncertainty in beam energy in terms of steep dose gradients.*

Materials and methods: *In this work a Monte Carlo (MC, EGS4) simulation for dosimerty study was performed for the 6MV home made SRT unit of the University Hospital of Patras (Hellas). The results were compared with conventional small field dosimetry techniques such as ionization chamber, TLD's, and films (conventional and radiochromic). Hence, a comparison of many of the dosimetric techniques currently being used in small field dosimetry was attempted.*

Results: *It was shown that all techniques are in reasonable agreement (within ± 2%) and that Monte Carlo can be used as a reliable reference for the dosimetry of the SRT beams, especially where lateral electronic equilibrium does not exist, as long as accurate simulation can be achieved.*

Conclusion: *This study is only limited by the insurance of accurate simulation of the linear accelerator, which can be a difficult task since it is limited by the availability of the manufacturer's designs and the availability of computers and computer time for adequate runs, but it could become a useful tool for Monte Carlo simulations, as it contains detailed analysis of the run parameters and component modules selection.*

Key words: Monte Carlo, radiosurgery, small field dosimetry, stereotactic radiotherapy

Introduction

The aim in the stereotactic irradiation technique (Stereotactic RadioTherapy, Stereotactic RadioSurgery, SRS-SRT) is to externally deliver a relatively large radiation dose to an intracranial volume, with extreme precision and accuracy in positioning.

Accurate dosimetry for narrow beams is very important because it is essential that the position and dimensions of the field are precisely matched, and a precise dose is released to the target volume. For SRS/SRT beams lateral electronic equilibrium does not exist in a large proportion of the beam, hence accurate dosimetry is more difficult than with conventional radiotherapy beams.

In the published literature most data acquisition in SRT/SRS is based on diode, film, and partly on thermoluminescence dosimetry [1-4]. These detectors are energy and dose rate-dependent and moreover the film and TLD exhibit non-reproducibility and depend on processing conditions [2].

On the other hand Monte Carlo simulation has proven to augment the dosimetric information where

Received 30-08-2004; Accepted 24-09-2004

Author and address for correspondence:

Ioannis M. Tsougos, MSc
Department of Medical Physics
University Hospital of Larissa
P.O. Box 1425
411 10 Larissa
Hellas
Tel: +30 2410 682056
Fax: +30 2410 670117
E-mail: jtsoug@med.uth.gr

measurements are less reliable or not possible. They are in principle not affected by difficulties due to detector resolution and lateral electron disequilibrium, as in the case of dose measurements.

A comprehensive data set for a 6MV SRS accelerator was provided by Heydarian et al. [2], obtained by measurements with various detectors as well as Monte Carlo simulations. Specific photon spectra were not given, although mean values of the photon energy were reported. Verhaegen et al. [5] modelled a dedicated 6 MV SRS unit using the Monte Carlo code. Their dosimetric parameters were based on the actual photon and electron spectra in each individual cone. They showed that photon spectra are qualitatively not much influenced by the field diameter [6].

In this work, the home made SRT unit [7,8], based on a Electa SL75 linear accelerator, is simulated using the BEAM-OMEGA Monte Carlo code [9]. Calculated and experimental data are compared.

Narrow beam dosimetry and problems faced

The dosimetry of small fields is complicated mainly by two factors: 1. The lack of equilibrium in lateral charged particles which leads to steep dose gradients in the typical SRT penumbra region; and 2. The relationship between detector size and field dimension.

Electronic disequilibrium consequences

For SRT collimators, which define small circular fields, the radius can be smaller than the range of the electrons for the photon beam used. In these small fields every point, even in the center, is close to the edge and lateral electronic disequilibrium may exist everywhere in the field.

Bjangard et al. [10] found that full electronic equilibrium was not achieved in the center of any beam (for a 6 MV linear accelerator) with a full width at half maximum less than 3 cm in diameter. Hence, ionization chambers are inadequate [2] for SRT dosimetry mainly because of their relatively large sensitive volumes, particularly when electronic disequilibrium exists across the whole field.

The existence of this disequilibrium has several consequences:

– As the collimator radius is reduced, the output factor drops dramatically,

– The crossbeam profile may be flat only over a small fraction of the full width at half maximum (FWHM)

– The dependence of the output, or dose rate at a point on the central axis, on the source to point distance (SPD) may not follow the inverse square law for large values of SPD. Thus the dose rate on the central axis increases more rapidly with SPD than the inverse square law would predict.

Detector's size

One of the most important criteria in the choice of detector in narrow field dosimetry is the detector's size. It must be small enough to minimize perturbations of the particle fluence, but large enough to be subjected to a large number of interactions so that it will yield a signal that can be read with precision. In the case of an inappropriate detector or experimental geometry, there might be a significant dose fall off, within the sensitive volume from the center to the periphery of the detector, hence complicating the interpretation of central axis measured dose values.

Additionally, when making measurements away from the central beam axis, the detector might not be able to resolve correctly the existent steep dose gradient due to lateral electronic disequilibrium. It is obvious that the choice of the detectors depends on the quantity that needs to be measured, and that quantity can be either central axis dose measurements or beam profiles-dose distributions.

Beam profiles and central axis dose measurements are required as input data for the treatment-planning computer. Accurate determination of these parameters leads to accurate determination of the three-dimensional dose distribution produced by the treatment planning system.

As already mentioned, lateral electronic disequilibrium and steep dose gradients are characteristics of small SRT beams and obviously ionization chambers, because of their large sensitive volumes, are not quite suitable even placed parallel to the beam-axis. Therefore, small chambers with sensitive volumes < 0.1 cm^3 are generally used for absolute dose verification. A dosimetry system consisting of an electrometer, an ion chamber, and connecting cables may exhibit charge leakage. Since chamber sensitivity is proportional to volume, the effect of leakage on the measured charge is relatively greater for small chambers [4].

Film dosimetry could be a preferred technique in the dosimetry of these very small fields, but film is energy-dependent and also suffers from variations in the film coating and processing conditions which make it somewhat unreliable.

The use of radiochromic film may overcome some of the problems associated with conventional

radiographic films. Better tissue equivalence, higher spatial resolution, and room light handling are the main advantages of radiochromic films. The disadvantage of these films is nonlinearity of the response for doses in the clinical range. To achieve acceptable precision (±2%) much higher doses are necessary (around 100 Gy).

Silicon diodes, because of the very small size of the sensitive volume (60 μm thickness and 2.5 mm width for Scanditronix p-Si), are the common choice in dosimetry of SRT beams [1,11,12]. However, energy, dose rate, and directional dependence of response are negative factors in this application.

Diamond detectors, because of the near tissue equivalence of carbon, should act as suitable detectors, although their dose rate dependence could affect the result. If corrected they produce better results than the more commonly used diode and film dosimetry techniques [2].

On the other hand, Monte Carlo simulations have been found very useful in calculating SRT parameters, where detector convolution, energy and dose rate dependence as well as lateral electronic disequilibrium can cause errors [13].

Field size dependence

Field size dependence, due to the stem effect or other causes, is magnified when measuring the output factor for a radiosurgery field by the drastic change in field size between the calibration field (in this case of stereotactic radiotherapy 8X8 cm) and the radiosurgery field [14-17]. If the radiosurgery field is so small that electronic disequilibrium exists in the center, this effect adds to the field size dependence. If the detector response depends on photon energy, this may also add to the field size dependence, because the contribution of low energy scattered photons to the dose at the center of the field, decreases rapidly as the field size drops below a few centimeters.

A summary of the dosimetric techniques used in small field dosimetry, with their advantages and disadvantages is presented in Table 1.

Materials and methods

SRT unit

In the present study experiments were carried out in the home made stereotactic unit of the University Hospital of Patras [7]. The Unit is mounted on an Electa SL75 6MV accelerator, utilizing a couch mount for the docking of the immobilization frame to the treatment machine.

The mechanical accessories, in the form of additional collimating assembly, that were constructed for the conversion of the conventional unit to a stereotactic one, and were fitted on the linac's head are presented in Figure 1.

Monte Carlo simulations

The Electa SL75 linear accelerator and the additional collimating assembly used for SRT were accurately modeled using the BEAM 99/EGS4 code [9].

Table 1. A summary of the dosimetric techniques used in small field dosimetry

Dependences	*Diamond Detector [15]*	*Ionization Chamber [4,14,16]*	*Pinpoint Ion. Chamber [14]*	*Radiochromic Film [18,19]*	*Conventional Film [18,19]*	*TLD [6]*	*Silicon Diode [15]*
Dose rate	medium	medium	medium	medium	high	low	medium
Field size	low	high	low	medium	high	medium	low
Energy	medium	medium	medium	medium	high	low	medium
Directional	low	medium	low	N.A.	N.A.	–	medium
Processing conditions	N.A.*	N.A.	N.A.	high	very high	N.A.	N.A.
Detector size	low	high	low	N.A.	N.A.	high	low
Reproducibility	low	low	low	high	high	high	low
Spatial resolution	medium	low	low	high	medium	medium	high
Response linearity	low	medium	medium	low	medium	medium	medium
Sensitive volume	small	large	very small	N.A.	N.A.	medium	very small

*Non-Applicable

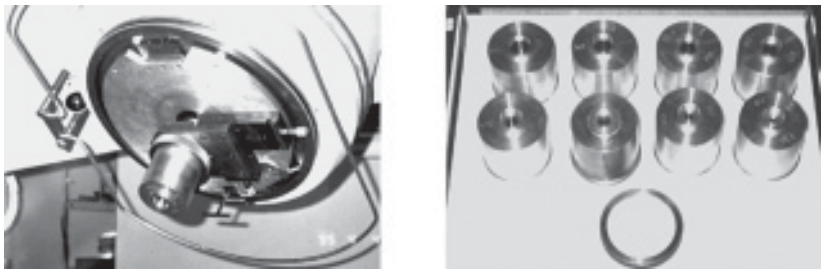

Figure 1. Collimating assembly and the eight additional stereotactic collimators.

In order to verify that our Monte Carlo calculations were accurate, we first simulated the Electa SL 75-5 Linear Accelerator for a 10X10cm field and obtained the PDD and Profile for the comparison with measured data. The results proved to be in satisfactory agreement, verifying that the Monte Carlo simulations can be used for dosimetric comparison. The results can be seen in Figure 2.

To reduce the run time as much as possible, and since there were eight collimators that needed to be simulated, the model was split into three steps. The first step was the simulation of the linear accelerator head, which would be common in all eight runs. The output of this simulation in the form of a phase space file (file containing information of the particle's energy, position coordinates, charge etc.) was then fed as the source in another run (second step) that simulated the additional collimating assembly. This was done eight times, adjusting the model geometrically for the eight additional collimators.

The third step for the analysis of the results and for the calculation of dose in Cartesian voxels, a 3-D phantom was designed using the DOSXYZ EGS4 user code [20,21]. Each DOSXYZ calculation read the corresponding phase-space file as input and provided output files containing all of the dose and fluence results of the simulation, which are then analyzed. The whole model is illustrated in Figure 3. The simulation can be summarized in Table 2.

Hence the first step of modellization was the simulation of the Electa SL75 linear accelerator. The model depicted in Figure 3, step 1, comprises the Target, Primary Collimator, Flattening Filter, Ionisation Chamber and the Jaws. All accelerator components were modelled as accurately as possible, based on information provided by the manufacturer (ELEKTA Medical Systems). The light field mirror was not included since it consists of a very thin layer of low atomic number material, and consequently does not affect significantly the photon beam [22]. The second step would then be to simulate the additional collimating assembly.

All Component Modules (CMs) are included in the BEAM/EGS4 Users Manual [9].

For every component module, the following parameters were set to:

E_{CUTIN} (i.e. the min. electron energy) = 0.521 MeV, if the energy of an electron drops below 0.521 MeV, the electron is no longer tracked and its energy is deposited in the current region.

P_{CUTIN} = 0.01 MeV respectively for photons.

ESAVE = 3.0, the maximum energy that a par-

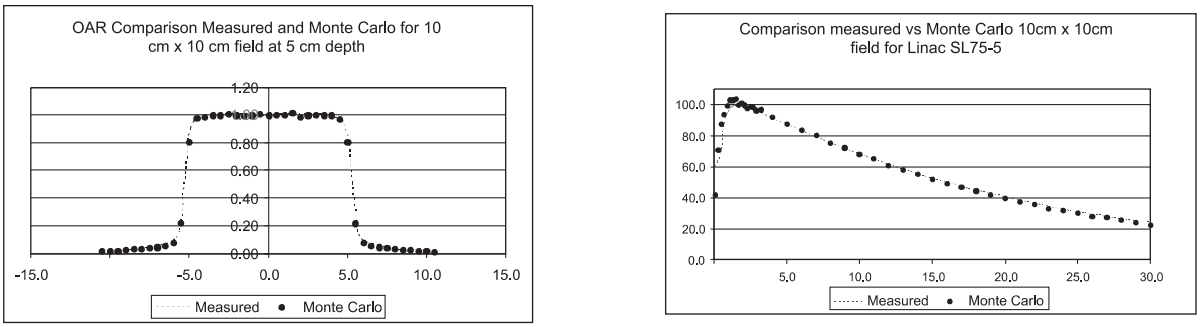

Figure 2. The Electa SL75-5 linear accelerator Monte Carlo simulations of the PDD and Profile in a 10 cmX10 cm field, and comparison with measured data.

Table 2. The whole model simulation summary

Component Modules	*Specifications*	*Steps*
Target	Slab of 4 cm width and 0.3 cm thickness Tungsten equivalent, density of 19.30 g/cm^3 E_{cutin}=0.521, P_{cutin}=0.01 MeV	
Primary Collimator	Stuck of truncated cones Materials: Inner 1.205X10^{-3}, Outer 17.5 g/cm^3	
Flattening Filter	Stuck of truncated cones Materials: Inner 1.205X10^{-3}, Outer 17.5 g/cm^3	First step of simulation
Ionization Chamber	Slab of 2 cm thickness Material: water 1 g/cm^3	
The Jaws	Set of paired bars in the X and Y orientation Material: Tungsten 19.3 g/cm^3	
Air	Slab with thickness depending on the SSD Material: Air, 1.205X10^{-3}, g/cm^3	
Additional Collimating Assembly *Metallic plate* *Pre-collimator* *Holder for additional collimator* *Additional collimator*	One single component module. Stuck of truncated cones coded as three regions. Materials: Air, 1.205X10^{-3} g/cm^3, Lead 10.5 g/cm^3	Second step of simulation
DOSXYZ Phantom	10 cm X 10 cm X 10 cm square comprised by 1 cm voxels everywhere except for the central region of the beam where the voxels were defined to be 0.2 cm	Third step of simulation

ticle can have for range rejection to be considered is 3.0 MeV. This parameter was introduced to minimize errors due to the assumption that any bremmstrahlung photons created when energy is deposited in a region do not leave that region.

For the Primary Collimator *CONS3R* is a stack of truncated cones coded as three regions of any dimensions the user might want to define. It can be used for any case with a cylindrical geometry, given that there exists only two radial regions. Hence four points (consider cylindrical geometry) were used to define this component module. Two for the z direction and two for the radius comprise a conical shape dividing the module into the inside and outside region (Figure 3).

Given the fact that the exact simulation of an ionization chamber is extremely complicated, the chamber was simulated by a slab of water of 2 cm thickness. By multiple tests it was proven that the interaction phenomena that would take place in the chamber are analogous to the slab of water considering its density and composition [23,24].

The second step was to simulate the additional collimating assembly (fitted into the Linac's face plate) consisting of a metallic plate, a pre-collimator, a holder for the additional collimator and 8 additional collimators.

The collimators ranged from 10 to 30 mm in diameter at the isocenter. The simulations were carried out with the same geometrical set-up, by changing the size of the collimator's diameter each time, keeping the rest of the conditions unchanged, thus ensuring homogeneity of the calculations.

The geometrical set-up used is shown in Figure 3, step2, as the 2D and 3D reconstruction of the collimating assembly. The phase space file of the simulation of an 8X8 cm^2 field at 100 cm was the source radiation entering the metallic plate of the collimator set-up.

In order to simulate the collimating assembly, it was decided that the best way to do it was by using one single component module, keeping the geometry as simple as possible, and at the same time preserving the geometrical accuracy. This was accomplished by the use of the CONS3R component module, since it can be used for any case with a cylindrical geometry (stack of truncated cones coded as three regions), given that there exists only two radial regions. Hence, eight points were used to define this component module. Four for the z direction and four for the radius comprise a conical shape dividing the module into the inside and outside region.

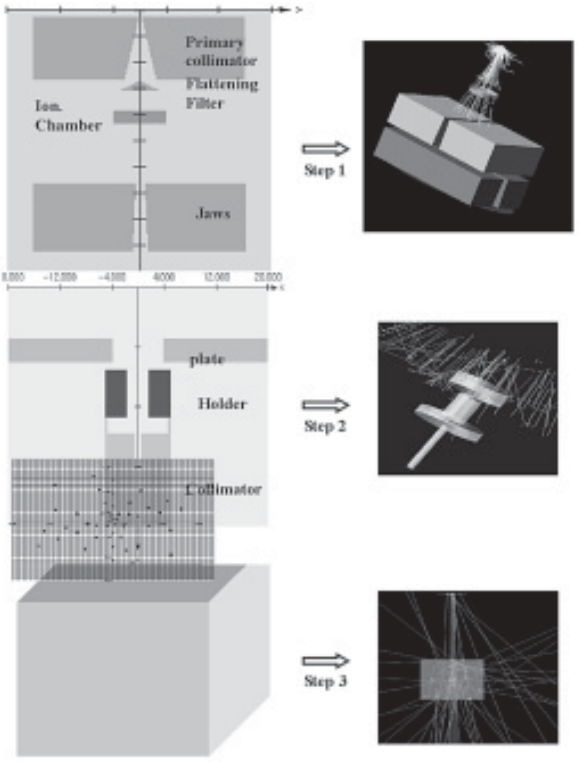

Figure 3. Schematic representation of the modeled accelerator-stereotactic collimator components using BEAM/EGS4, followed by the DOSXYZ phantom which, depending on the situation, was appropriately transformed into a system of Cartesian coordinates.

It is evident that this model of simulation contained virtually no fudge factor, since the only parameter that changed among the various collimators was their radius. The simulation was repeated eight times for the eight different collimators, using the same phase space file as the source radiation.

The main input parameters were set to the exact same values used for the first run, since they were selected on the basis of saving a great deal of computing time. Nevertheless, the fact that satisfactory results (by comparison to measured values) were obtained from the first simulation suggested that the selection of the main input parameters should be theoretically correct.

Finally, for the calculation of the dose distribution with the measured data, a 3-D water phantom was modeled using the DOSXYZ NRC Egs4 user code. It was divided into 30X30X5 slices in the x, y and z directions respectively, resulting in 4500 voxels of 0.2 cm^3 volumes each. The air gap between the collimators and the phantom was not taken into account since it was included in the phase space output. Each DOSXYZ calculation read the corresponding phase-space file as input, recycling it less than 9 times in order to provide an output in the form of a 3d-dose file. Central axis depth-dose curves were calculated in the 4X4 cm^2 region around the central axis.

Selection of run parameters

Selection of various run-time parameters for any Monte Carlo calculation can be very complex and often depends on what aspect of the results are most important and how many resources are to be consumed by the calculation. The BEAM code uses the PRESTA [9,14] algorithm for electron transport.

Lower values of AE, which is the lowest total energy of secondary electrons, simulate more interactions and create more realistic energy-loss straggling distributions. If studying energy spectra, it is important to use a low value of AE (0.521 MeV), but if calculating depth-dose curves, much higher values are completely accurate. Hence we performed test simulations and it was shown, that using an AE value of 0.521 MeV instead of 0.700 MeV when using a value of ECUT = 0.700 MeV has virtually no effect on the results shown, but increases the computing time by approximately 30%. It also significantly affects the high-energy electron fluence spectrum and thus the lower value should only be used if energy spectra are of interest.

In order to save computation time it is advisable to introduce higher ECUT and PCUT values inside some of the component modules of the accelerator (Primary Collimator, Secondary Jaws, etc.). The electrons that will enter inside these component modules have a very small probability to exit and even if they exit they will have lost most of their energy and will deposit the rest in the next module in their path. Therefore, if those electrons that enter for example the primary collimator have ECUT = 0.521 MeV that means that they will loose 0.521 MeV after each interaction and since it most likely to never exit the primary collimator, the time to compute their path is useless for our simulation. Hence, if one sets the ECUT = 2.0 MeV reduces the number of interactions the electrons will undergo in such component modules and saves computation time. Nevertheless, for therapy beams this can be quite high since low energy electrons contribute little to dose in phantom, and so it was set to 0.521 MeV.

Main inputs

The main input parameters determine the output of the whole run, and at the same time play a significant role in the duration of the run, as they can

Table 3. Main input parameters

Main Inputs	*Options*	*Specifications*
Latch option	1. Non- inherited latch 2. Inherited latch set by passage 3. Inherited latch set by interaction	It means that latch values are passed on to secondary particles from the primaries that created them.
Bremsstrahlung splitting	1. None 2.Uniform 20 photons 3. Selective	The number 20 was selected as the optimum in terms of CPU time, from trails in steps of 5 from 5 to 50 interval.
Splitting	Electrons and photons 10 times at the jaws	It is not generally recommended since it may introduce correlations, which may not be desirable. Nevertheless the value of 10 was chosen as it was proved to be statistically correct.
Estepe	No estepe control	Determines the length of time required for simulation and the detailed accuracy. Hence it was controlled by the PRESTA algorithm directly.
Smax	5 cm	This value was found to give adequate lateral scattering for electrons going through air.
Ecutin	0.521 MeV	For therapy beams this can be quite high since low energy electrons contribute little to dose in phantom.
Pcutin	0.01 MeV	The exact value of Pcutin is not critical in the sense that low values do not affect the run time dramatically.
Rayleigh Scattering	Not included	For high energy electron and photon beams Rayleigh processes are negligible and including it in the simulation would increase CPU time unnecessarily.

save a great deal of computing time if chosen wisely. Using Rogers' BEAM/EGS4 Manual, the main input parameters for this specific simulation are summarized in Table 3.

In bremsstrahlung splitting the energy of the primary electron is decremented by the energy of just one of the photons. This must be done in order to preserve the effects on energy straggling. This means that energy is not conserved on a given history (the energy would have to be decremented by the average energy of the photons created) but it is conserved on average over many histories [9].

Also it was possible to reduce the CPU time while still preserving the variance reduction advantages of bremsstrahlung splitting by using a Russian Roulette technique with the electrons generated by the split photons. Russian Roulette is implemented by choosing a random number for each electron created by a split photon at the time of interaction, and comparing this number to a threshold of $1/\chi$. If the random number is less than the threshold, the electron survives and has its weight increased by a factor of χ. Otherwise, the electron is eliminated. Hence, it was set for electrons and higher order bremsstrahlung photons.

The choice of SMAX (the maximum step of a particle before interacting) depended on the lengths of air gaps in the accelerator being simulated. If SMAX would be large relative to the average length of air gaps, then the details of particle scatter in air would be missed. On the other hand, a very small SMAX would suggest an unnecessary number of steps taken through air gaps, increasing the CPU time required.

BEAM offers an option where the user can force photons to interact in specified Component Modules (CMs) within a simulation. One of the main purposes of implementing this option was to study the generation of contaminant electrons in the photon beam. This option is useful for improving statistics of scattered photons when photon interactions are not many (e.g. in thin slabs of material or in material with low density).

A photon forced to interact in a CM is "split" into a scattered photon whose weight is equal to the probability of interaction, and an unscattered photon carrying the remaining weight. The unscattered photon proceeds as if an interaction did not take place, and it cannot be forced to interact any more within the specified forcing zone, which can consist of one or several component modules. However, once the unscattered photon gets out of the forcing zone, it

may interact again depending on the sampled pathlength. The scattered photon can be forced again in the forcing zone depending on how many interactions are allowed to be forced [9,23].

It was specified so that forcing would start after the first interaction of the particle, and right after exiting the Jaws component module, hence in air because of low density.

The simulations were carried out in two personal computers using a Pentium 833 MHz and a Celeron 700 MHz processor running Linux. The field size used for any experiment carried out in the stereotactic unit was 8X8 cm. The number of particle histories for the simulation of the Linac was $20X10^6$, yielding $18X10^6$ particles in the scoring plane. The initial particles were electrons and the incident kinetic energy 6.06 MeV. The beam radius was 0.4 cm. The initial random numbers were 19 and 53. Various energies were used in order to find the one that best describes the dosimetric data (percent depth dose and Off – axis – ratios) for the SL-75 Linear accelerator in the range 5.7 to 6.3 MeV. The energy of 6.06 MeV was found as the one that gives the best dosimetric data when compared to the measured ones.

For the simulation of the stereotactic collimators the number of histories were $50X10^6$. The maximum kinetic energy was 6.056 MeV and the minimum 0.010 MeV. The total number of particles in the scoring plane (i.e. below the jaws) was 8219403 with 8215140 being photons.

Thermoluminescense and ionisation chamber dosimetry

- *TL dosimetry*

Hartmann et al. [25] stated that for central axis measurements the detector size should be the 1/3 of the field size used. Until now the TLD's dimension used for such measurements is of the order of 3 mm. Rice et al. [1] also recommended a detector size of 1 mm (or less) for dose profile acquisition. For the practical application of these dosimeters for the determination of dose profiles and the verification of dose distributions produced by the complete stereotactic irradiation scheme, a phantom for their accommodation was constructed [19,26].

The central region of the phantom is a circular plexiglas disk of 10 cm in diameter and 1 cm thickness, inserted in a centrally located hole in a plexiglas slab of 30X30X1 cm^3. The slab that accommodates the dosimeters is attached from both sides to plexiglas slabs using plastic inscribed screws. The whole assembly can be inserted at any depth of a standard 30X30X1 cm^3 plexiglas phantom.

The holes in the centrally located disk area were machined vertical to the large surface of the disk in a circular area of 4.6 cm in order to cover the whole range of the additional collimators of the Stereotactic Unit.

In the centrally located area of 4.6 cm in diameter, there is a dense network of holes (Figure 4). Each hole is placed on increasing, by steps of 1 mm, concentric circles in diameter at angles 15, 30, 60, 90, 115, 135, 164^0 defined from the transverse axis passing from the centre of the circular disk.

In order to be used in SRT/SRS, the phantom should provide high spatial resolution due to the steep dose gradients involved in the technique. On the other hand, field perturbation due to the presence of a dense array of TLDs should to be kept as low as possible.

Hence it consists of an array of holes to accommodate up to 71 TL dosimeters to allow the assessment of dose distribution in circular fields with 1mm spatial resolution with minimal field perturbation. The phantom in its actual form can be seen in Figure 4.

A total of 200 cubical LiF:Mg,Ti,… dosimeters (1X1X1 mm^3) by Harshaw/Bicron were used. Before each experiment, TLDs were annealed at 400° C for 1h, followed by a 100° C temperature hold for 2h, using a pre-programmed PTW TLDO oven. Prior to the readout, the dosimeters were annealed at 100° C for 10 min. The thermo-luminescence signal was measured by a Harshaw 2000A and 2080B reader (Medical Physics Lab. of Ioannina, Ioannina, Hellas).

The circular disk was used to accommodate the TLDs. It was inserted in the hole of a 30X30X1 cm^3 plexiglas plaque, and the assembly of the disk with the plaque was used as a part of the standard 30X 30X30 cm^3 plexiglas phantom.

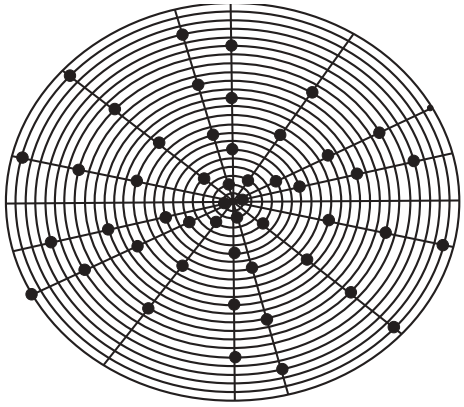

Figure 4. The Phantom in its actual form.

Holes of the circular disk that were not in use were filled with 6 mm plexiglas plugs, while the cubical TLDs were supported by 5 mm plexiglas spacers.

The dose profiles were obtained at 4.3 cm depth in plexiglas (5 cm water equivalent depth) at the isocenter, with 5 cm plexiglas backscattering material. Two experiments were performed for each collimator and the number of TLDs used varied depending on the field size. They were simultaneously irradiated at a dose of 75 MU and the profiles were obtained by averaging the dose from corresponding positions in the phantom.

Table 4. The characteristics of the ionization chambers

Chamber	*Thimble (0.1 cm³)*	*Marcus parallel plate*
Type	M23344	M23343
Sensitive volume	0.1 cm^3	0.04 cm^3
Polarization voltage	max 500V	max 300V
Wall material	$C_5H_8O_2$	CH_2
Wall thickness	1.75 mm	0.03 mm
Weight / unit area	210 mg/cm^2	60 mg/cm^2
Cavity diameter	5 mm	30 mm
Cavity length	12 mm	2 mm
Central electrode length	1 mm	–

- *Ionisation Chamber dosimetry*

The basic dosimetric data were also assessed in a 2D water phantom (PTW), using a thimble ionisation chamber (PTW 23344), 0.1 cm^3 in sensitive volume. The determination of the effective centre of the chamber was based on measurements acquired by a Marcus plane-parallel ionisation chamber (PTW 23342) of 0.04cm^3 in sensitive volume. The characteristics of the ionisation chambers are summarized in Table 4.

The dose measurements were performed in a 2D water phantom and taking into account the dimensions of the sensitive volume of the chamber (internal diameter 5 mm and 12 mm in length), the measurements were obtained in two positional configurations of the chamber, with its longitudinal axis parallel and vertical to the central beam axis [18]. However, for the comparison of the dose profiles and PDDs with Monte Carlo and TLDs the parallel configuration is used, since both configurations are in reasonable agreement. Also the determination of the effective center of the chamber was implemented for the parallel configuration, as well as centering and alignment of the chamber with the central beam axis and of the collimation assembly with the center of the irradiation field.

Results-Discussion

The Monte Carlo results from the simulation of the Electa SL 75 linear accelerator are presented in Figure 5. The phase space data obtained in the scoring region right below the jaws provide histograms of

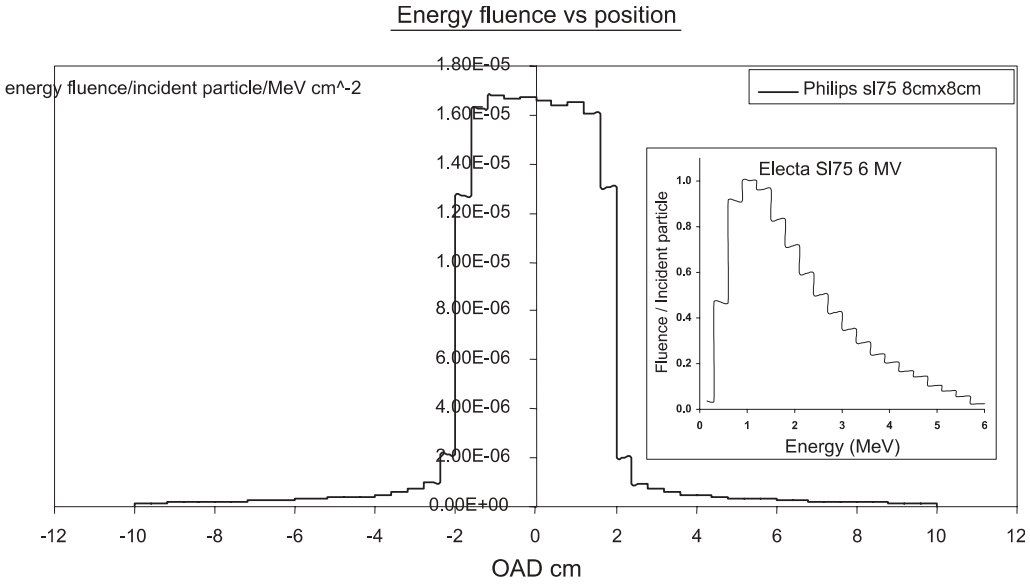

Figure 5. The energy profile and the spectral distribution of the Electa SL75 linac as produced by the phase space file.

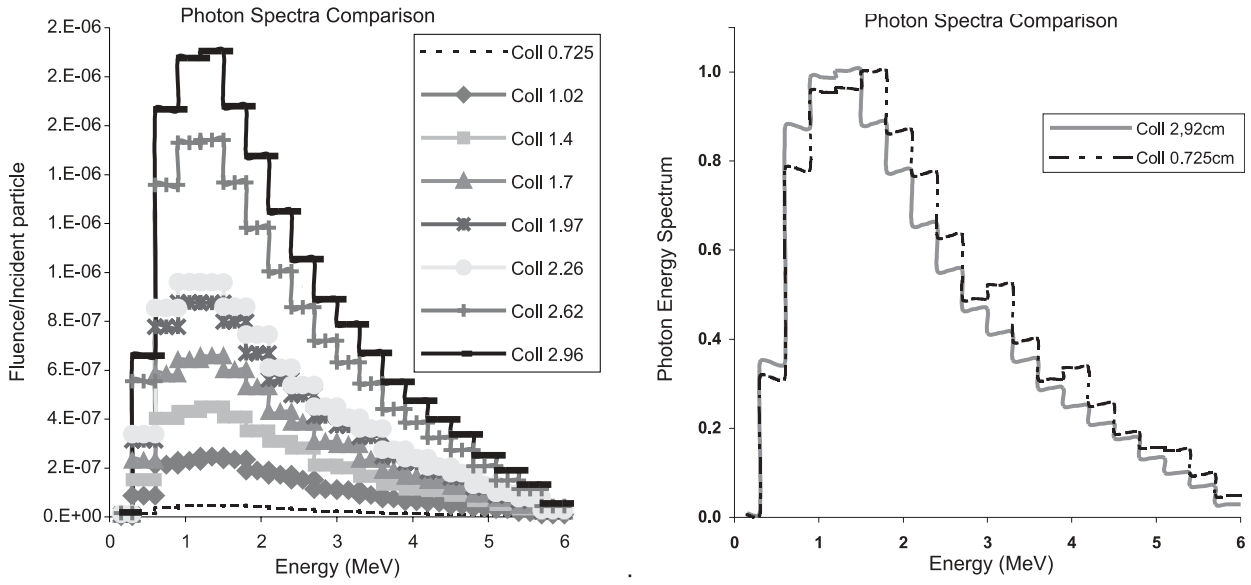

Figure 6. Spectral distributions for the complete range of collimator diameters, from 0.725 cm to 2.92 cm and normalized Photon Spectra Comparison for the two 'extreme' (in diameter) collimators.

the accelerator's energy profile and its spectral distribution (fluence/incident particle *versus* energy). The analysis of the phase space files from different collimators gives a comparison of spectral distributions for photons. In Figure 6 the photon spectra comparison for all the collimators as well as the two 'extreme' (in diameter) collimators is presented, while the respective mean energies distributions are demonstrated in Figure 7.

Results of the Monte Carlo calculated PDDs and dose profiles, compared with the PDDs and dose profiles of the two different dosimetric techniques for the two extreme collimator apertures are presented in Figures 8 and 9, respectively.

The analysis of the phase space output at the exit of the accelerators jaws gave rise to the energy profile depicted in Figure 5. For all stereotactic unit measurements the field size was set to 8x8 cm. A first look at Figure 6 can be misleading because it seems like the field size is only 4X4 cm. This is due to the fact that the phase space file's scoring region is directly below the jaws and not at 100 cm. It is those

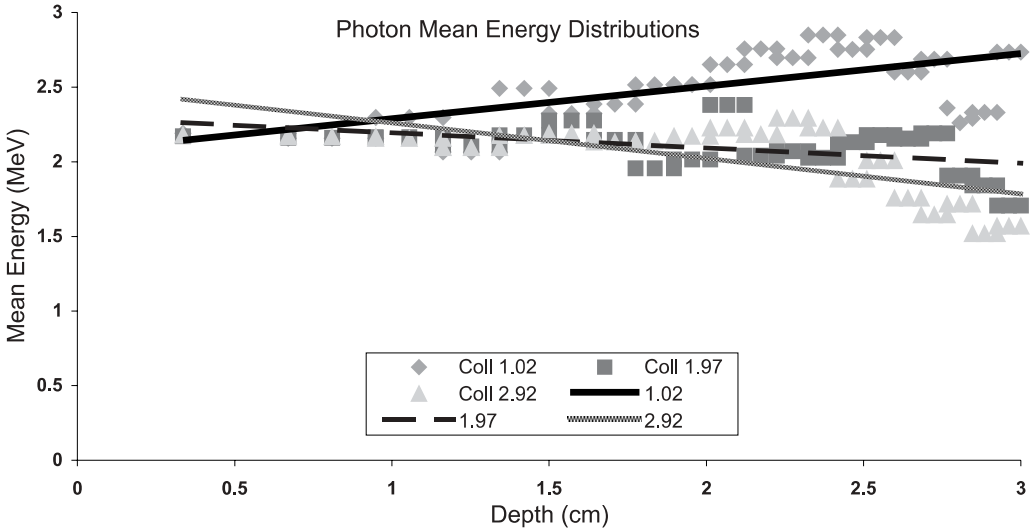

Figure 7. An indicative comparison of photon mean energy distribution.

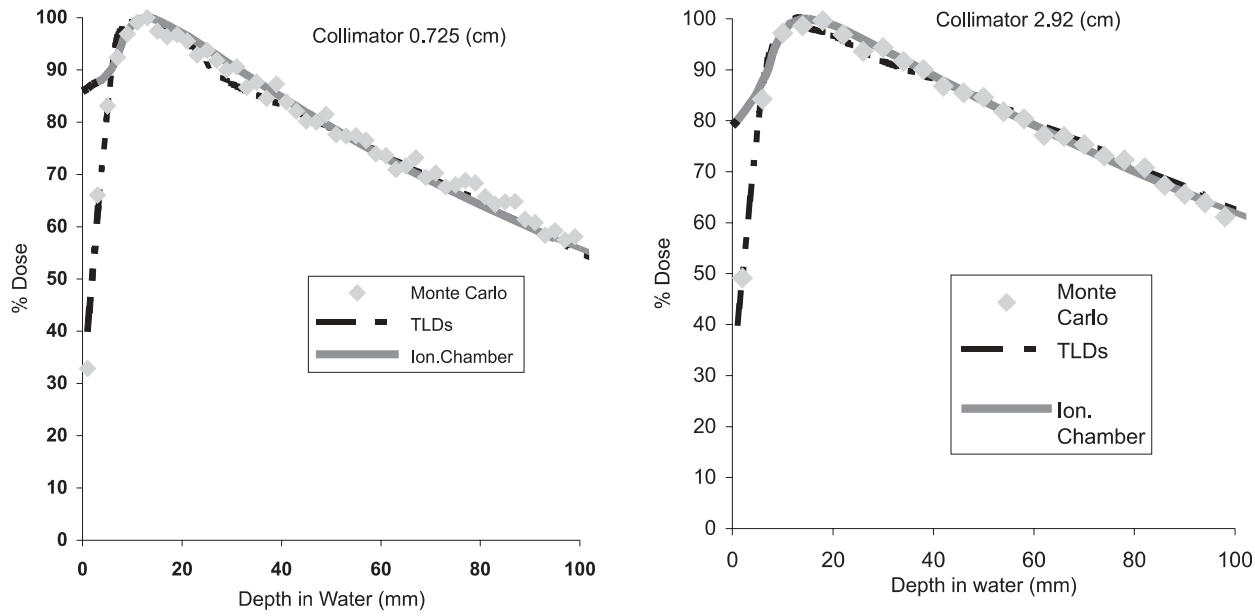

Figure 8. PDD comparison of the three different dosimetric techniques. Collimator diameters 0.725 and 2.92 cm.

settings of the accelerator that yield a field size of 8X8 cm at 100 cm.

The maximum statistical uncertainty in the phase space file does not exceed 3%. Most particles in the file have energy of 1 MV (Figure 7), while the mean energy of photons is approximately 2.13 MV (phase space analysis).

In Figure 6, where the spectral distributions for the complete range of collimator diameters from 0.725 cm to 2.92 cm are shown with detailed analysis, one can note an increase in the average photon energy with decreasing collimator diameter. This can be explained because with the opening of the collimator diameters more internally scattered and therefore softer photons participate in the fluence.

The previous statement is verified by the comparison of the photon energy spectra for the two "extreme" in diameter collimators also in Figure 6. The fluence was normalized to unity in order for the two, to be comparable. It is clear that there is a 'shift' of the

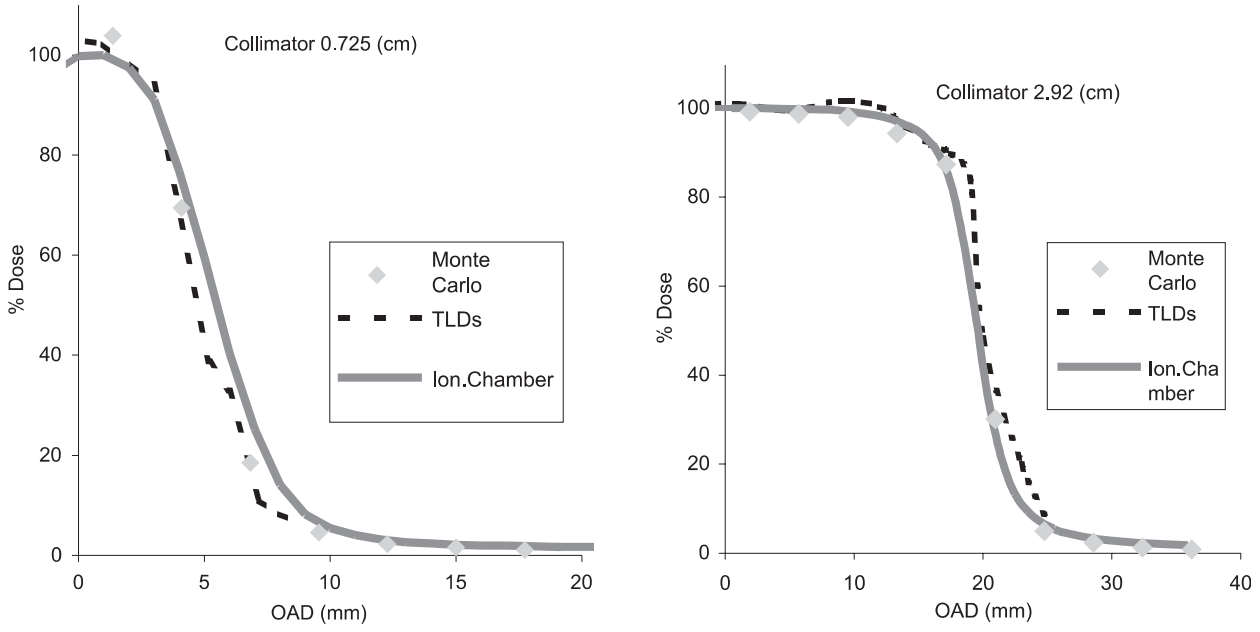

Figure 9. Dose profile comparison, collimator diameters 0.725 and 2.92 cm.

smaller collimator to higher energies. This was to be expected since it is the result of less scatter contribution in the smaller collimator. In other words, the hardening of the primary beam dominates in the smaller collimator opening. This is also very well illustrated in Figure 7 in terms of photon mean energy distribution. In this Figure it is verified that the photon energy spectra for the broad beam are softer than those of the narrower beam. It can be seen that the mean energy of narrower beams shows a larger increase with depth, as the result of the reduced scatter contribution, i.e. the hardening of the primary beam dominates.

The indicative comparison of depth dose results for the two 'extreme' in diameter collimators with different techniques is shown in Figure 8. The depth doses are in reasonable agreement among the three different techniques for the whole range of the collimators. Nevertheless it can be seen that Monte Carlo calculations are in better agreement with the TLD measurements for the complete range of collimator diameters, whereas the Ionization Chamber measurements tend to coincide as the collimator diameter increases. This is a first indication that ionization chambers might be inadequate for very small fields, mainly because of their relatively large sensitive volumes. Nevertheless the agreement between the Monte Carlo technique and the TLDs and ionization chamber confirms the validity of the photon energy spectrum and EGS4 simulations. This means that the Monte Carlo generated depth doses for small SRT fields, where lateral electronic equilibrium does not exist, can be used as reliable references for dosimetry purposes.

The comparison of the Monte Carlo calculated and measured Off Axis Factors for the two 'extreme' in diameter SRT collimators is illustrated in Figure 9. As it can be seen from these Figures, Monte Carlo profiles (with standard deviation better than 1.3%) are in reasonable agreement with the other two techniques. They have almost the same FWHM as the experimentally obtained profiles, but there is a general inconsistency in the penumbra widths. The FWHM and penumbra widths (80-20%) for all dosimetric techniques are summarized in Table 5.

The Table shows that the dosimetric techniques applied resulted to almost the same FWHM, but in different penumbra sizes. The penumbra size *versus* collimator diameter graph in Figure 10 shows that the penumbra widths obtained by Monte Carlo calculations and by ionization chamber dosimetry are closer together and have a slight linear increase with the collimator diameter. On the other hand TLD dosimetry penumbras contain a substantial difference from the other two, especially for the lower half of the collimator diameter range. Furthermore, these values vary linearly with collimator aperture.

Heyderian et al. [2] reported on Off Axis Ratios (OAR) obtained with a diamond detector, a diode, films and Monte Carlo techniques, at a depth of 6 cm. They found that the profiles obtained by Monte Carlo calculations had almost the same FWHM as their experimental profiles but different penumbra widths, which is in complete agreement with the results of this study. Nevertheless, the absolute values have considerable differences, but they cannot be compared since the conditions are not identical (differences in the experimental arrangement, different collimating assembly) nor the collimators diameters are the same, and hence these can cause serious deviations.

In Figure 11 the collimator size dependence of the PDD, assessed with Monte Carlo, is given for 3, 5 and 9 cm depths. It is evident that PDDs obtained with Monte Carlo calculations have a linear increase with collimator aperture for these depths.

Figure 12 shows that the surface PDDs for the

Table 5. Summary of the FWHM and 80-20% penumbra width for the complete range of collimators and for different techniques

	Monte Carlo		*Ionization Chamber*		*TLD*	
Collimator Diameter (mm)	*FWHM*	*80-20%*	*FWHM*	*80-20%*	*FWHM*	*80-20%*
10	10.1	3.5	10	3.8	9.9	2.8
14	14.6	4.25	14.3	4.1	14.3	2.6
19	20	4.0	19.5	4.0	19.0	3.2
23	24	4.5	24.2	4.2	23.3	4.0
27	28.6	4.2	27.8	4.4	28.4	4.0
31	31.8	4.6	32	4.1	31.4	3.6
36	38	4.5	37.5	4.4	37.2	3.5
40	40.2	4.1	41.2	4.6	40.8	4.1

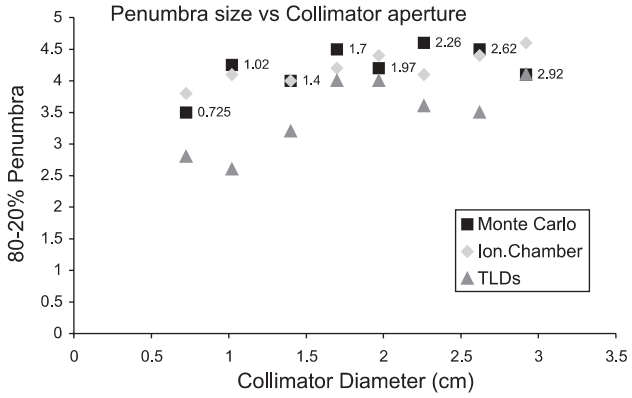

Figure 10. Penumbra size vs. collimator diameter.

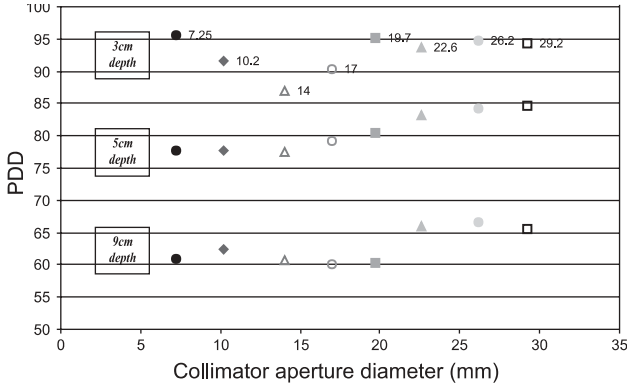

Figure 11. Monte Carlo calculated, collimator size dependence of the PDDs for 3.5 and 9 cm depth.

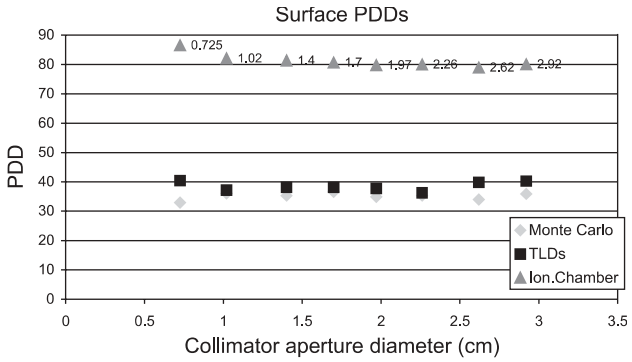

Figure 12. Surface PDD vs. collimator aperture for the different dosimetric techniques.

TLD and Monte Carlo techniques are in reasonable agreement and both are almost independent of the stereotactic field size. The PDDs of the ionisation chamber technique are appreciably larger from the other two.

For typical stereotactic fields diamond detectors result in surface PDDs of about 40% [2], which is in very good agreement with the value obtained with Monte Carlo in the present study.

Conclusion

It is a fact that in the absence of electronic equilibrium the detectors responses cause errors in dose calculations. For the case of narrow beams this is especially due to the detector size dependence and to tissue non-equivalence. According to Heydarian et al. [2] lateral electronic equilibrium will generally be achieved when the radiation field diameter is at least twice as big as the maximum lateral range of the primary electrons, which in turn is approximately equal to the depth of the maximum dose (dmax). On the other, hand Wu et al. [27] state that for very small fields (narrow beams), where lateral electronic equilibrium does not exist, there is lack of the lower-energy electrons which otherwise could have reached the central axis.

The bottom line is that in order to avoid over- or underestimation of the actual treatment volume, in an area with increased importance as in small fields, there is a need for the determination of an accurate dosimetry technique [14, 28-30].

In this study Monte Carlo techniques were evaluated and it was shown that they can be used as reliable references for the dosimetry of the SRT beams, as long as accurate simulation can be achieved, especially where lateral electronic equilibrium does not exist.

The drawbacks are:

a) The insurance of accurate simulation of the machine, which can be a difficult task since it is limited by the availability of the manufacturer's designs of the machine.

b) The availability of computers and computer time for adequate runs.

c) The 'assumption' that the accelerator and additional collimating assembly remain unchanged with time.

In other words, it is obvious that Monte Carlo techniques can be used for the dosimetry of narrow beams, but it would be safer to have another dosimetry technique to be used as reference in order to verify the accuracy of the simulation.

References

1. Rice RK, Hansen JL, Svenson GK, Sibbon RL. Measurements of dose distributions in small beams of 6 MV x-rays. Phys Med Biol 1987; 32: 1087-1099.
2. Heydarian M, Hoban PW, Beddoe AH. A comparison of dosimetry techniques in stereotactic radiosurgery. Phys Med Biol 1996; 41: 93-110.
3. AAPM. A protocol for absorbed dose from high energy photon beams TG. Med Phys 1983; 21: 10.

4. Leybovich LB, Sethi A, Dogan N. Comparison of ionization chambers of various volumes for IMRT absolute dose verification. Med Phys 2003; 30: 119-123.
5. Verhaegen F, Das IJ, Palmans H. Monte Carlo dosimetry study of a 6MV stereotactic radiosurgery unit. Phys Med Biol 1998; 43: 2755-2768.
6. Kalef-Ezra J, Bazioglou M, Theodorou K, Kappas C. A phantom for dosimetric characterization of small radiation fields: design and use. Med Dosim 2000; 25: 9-15.
7. Kappas C, Theodorou K, Kardamakis D et al. Design, Construction and Installation of a New Stereotactic System for Single Dose and Fractionated Radiotherapy. Physica Medica 1997; 13: 123-128.
8. Theodorou K, Kappas C, Tsokas C. A new non-invasive and relocatable immobilization frame for fractionated stereotactic radiotherapy. Radiother Oncol 1998; 47:313-317.
9. Rogers DWO, Faddegon BA, Ding GX, Ma CM, Mackie TR. BEAM: A Monte Carlo code to simulate radiotherapy treatment units. Med Phys 1995; 22: 503-524.
10. Bjarngard BE, Tsai JS, Rice RK. Doses on the central axis of narrow 6 MV x-ray beams. Med Phys 1990; 17: 794-799.
11. Beddar AS, Mason DJ, O'Brien PF. Absorbed dose perturbation caused by diodes for small field photon dosimetry. Med Phys 1994; 21:1075-1079.
12. Higgins PD, Sibata CH, Siskind L, Sohn JW. Deconvolution of detector size effect for small field measurement. Med Phys 1995; 22: 1663-1666.
13. De Vlamyck K, Palmans H, Verhaegen F, Thierens H. Dose measurements compared with Monte Carlo simulations of narrow 6 MV multileaf collimator shaped photon beams. Med Phys 1999; 26: 1874-1882.
14. Sanchez-Doblado F, Andreo P, Capote R et al. Ionization chamber dosimetry of small photon fields: a Monte Carlo study on stopping-power ratios for radiosurgery and IMRT beams. Phys Med Biol 2003; 48: 2081–2099.
15. Westermark M, Arndt J, Nilsson B, Brahme A. Comparative dosimetry in narrow high-energy photon beams. Phys Med Biol 2000; 45: 685–702.
16. McKerracher C, Thwaites D. Verification of the dose to the isocentre in stereotactic plans. Radiother Oncol 2002; 64: 97–107.
17. Duggan DM, Coffey CW. Small photon field dosimetry for stereotactic radiosurgery. Med Dosim 1998; 23: 153-159.
18. Theodorou K, Platoni K, Lefkopoulos D, Kappas C, Schlienger M, Dahl O. Dose-volume analysis of different stereotactic radiotherapy mono-isocentric techniques. Acta Oncol 2000; 39:157-163.
19. Bazioglou MA, Kalef-Ezra J, Kappas C. Comparison of dosimetric techniques for the assessment of basic dosimetric data of stereotactic fields. Physica Medica 2001;18:123-128.
20. Treurniet JA, Rogers DWO. DOSXYZ and BEAMDP GUI User's Manual. NRC Report PIRS (Rev A), 1999.
21. Ma C, Rogers DWO. BEAMDP Users Manual. NRCC Report, NRC, Canada 1996.
22. Lovelock DMJ, Chui CS, Mohan RA. Monte Carlo model of photon beams used in radiation therapy. Med Phys 1995; 22: 1387-1394.
23. Bielajew AF, Rogers DWO. PRESTA- The parameter reduced electron-step algorithm for electron Monte Carlo transport. Report NRCC/PIRS 0436, June 1994.
24. Bielajew AF. Fundamentals of the Monte Carlo method for neutral and charged particle transport. University of Michigan Publications, 1998.
25. Hartmann GH, Bauer-Kirpes B, Serago CF, Lorenz WJ. Precision and accuracy of stereotactic convergent beam irradiations from a linear accelerator. Int J Radiat Oncol Biol Phys 1994; 28: 481-492.
26. Bazioglou MA, Kalef-Ezra J. Dosimetry with radiochromic films: Technique and application. Physica Medica 1999; 15: 215.
27. Wu A, Zwicker RD, Kalend AM, Zheng Z. Comments on dose measurements for a narrow beam in radiosurgery. Med Phys 1993; 20: 777-779.
28. Komanduri M, Ayyanga R, Steve B. Do we need Monte Carlo treatment planning for Linac based radiosurgery?. Med Dosim 1998; 23: 161-167.
29. Andreo P. Monte Carlo techniques in medical radiation physics. Phys Med Biol 1991; 36: 861-920.
30. Solberg T, DeMarco J, Holly F, Smathers J, DeSalles AF. Monte Carlo treatment planning for stereotactic radiosurgery. Radiother Oncol 1998; 49: 73-84.